ACS OMEGA

Open Access

http://pubs.acs.org/journal/acsodf

Article

Synthesis and Anti-*Trypanosoma cruzi* Activity of 3-Cyanopyridine Derivatives

Brian W. Slafer,[⊥] Marco A. Dessoy,[⊥] Ramon G. de Oliveira, Maria C. Mollo, Eun Lee, An Matheeussen, Louis Maes, Guy Caljon, Leonardo L. G. Ferreira, Renata Krogh, Adriano D. Andricopulo, Luiza R. Cruz, Charles E. Mowbray, Jadel M. Kratz, and Luiz C. Dias*

Cite This: *ACS Omega* 2024, 9, 22360−22370

Read Online

ACCESS | Metrics & More | Article Recommendations | Supporting Information

ABSTRACT: Chagas disease (CD) is a parasitic neglected tropical disease (NTD) caused by the protozoan *Trypanosoma cruzi* that affects 6 million people worldwide, often resulting in financial burden, morbidity, and mortality in endemic regions. Given a lack of highly efficient and safe treatments, new, affordable, and fit-for-purpose drugs for CD are urgently needed. In this work, we present a hit-to-lead campaign for novel cyanopyridine analogues as antichagasic agents. In a phenotypic screening against intracellular *T. cruzi*, hits **1** and **2** were identified and displayed promising potency combined with balanced physicochemical properties. As part of the Lead Optimization Latin America consortium, a set of 40 compounds was designed, synthesized, and tested against *T. cruzi* intracellular amastigotes and relevant human cell lines. The structural modifications were focused on three positions: cyanopyridine core, linker, and right-hand side. The ADME properties of selected compounds, lipophilicity, kinetic solubility, permeability, and liver microsomal stability, were evaluated. Compounds **1**−**9** displayed good potency (EC_{50} *T. cruzi* amastigote <1 μM), and most compounds did not present significant cytotoxicity (CC_{50} MRC-5 = 32−64 μM). Despite the good balance between potency and selectivity, the antiparasitic activity of the series appeared to be driven by lipophilicity, making the progression of the series unfeasible due to poor ADME properties and potential promiscuity issues.

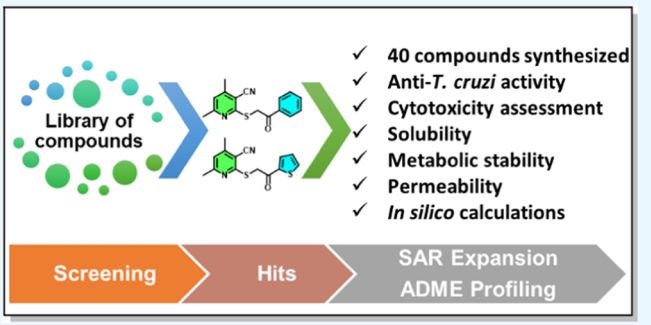

INTRODUCTION

Chagas disease (CD), caused by the kinetoplastid parasite *Trypanosoma cruzi*, is endemic in twenty-one countries in Latin America and is a major cause of chronic morbidity and mortality.[1] This disease is a serious public health burden in the region, and the Pan-American Health Organization (PAHO) estimates that 6 million people are infected and 70 million are at risk worldwide.[2] Due to the increasing movement of people between Latin America and other continents, CD is no longer confined to the Americas and can also be found in the USA, Europe, and some African, Eastern Mediterranean, and Western Pacific countries.[1] The disease evolves in two phases: the acute and the chronic; and although most infected people will remain asymptomatic, 20−30% will progress to the chronic stage and develop severe damage to the heart, digestive, and/or nervous systems.[2]

Only two antiparasitic treatments are currently available, the nitro-heterocyclic drugs benznidazole and nifurtimox.[3] Both drugs require long administration (30−60 days) and are poorly tolerated, limiting patients' adherence to the treatment and their broader use.[4] Fortunately, the recent success of the BENDITA trial,[5] reported a shorter benznidazole regimen being as efficacious as the standard treatment and possibly having a safer profile. Nevertheless, regarding drug discovery campaigns, all new chemical entities (NCEs) that have progressed for clinical trials in CD patients in recent years have failed.[6−8] These include promising CYP51 inhibitors posaconazole and fosravuconazole, which act by targeting the ergosterol biosynthesis pathway.[9] Thus, discovering and developing novel and chemically diverse NCEs that might act through novel mechanisms of action is imperative for controlling the infection.

Herein, we describe the hit-to-lead optimization of a novel cyanopyridine series. Initial hits TDR30139 and TDR26631 showed good potency and balanced properties for the hit identification stage, including no clear CYP51 inhibition (Figure 1). These hits were originated from the screening of 10,000 compounds at the University of Antwerp as part of the Lead Discovery for Infectious Tropical Diseases project by the

Received: February 27, 2024
Revised: April 14, 2024
Accepted: April 17, 2024
Published: May 13, 2024

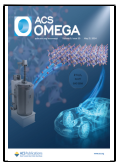

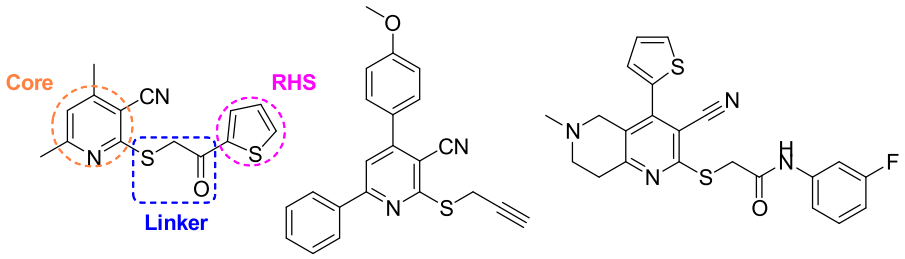

Targeted properties	TDR30139 (1)	TDR26631	PCBRO01-2472
T. cruzi IC_{50}	<5 μM	0.34 μM	2.9 μM	<0.1 μM
SI	>10	>28	>28	600
PAMPA	>1.5 10^{-6} cm/s	24.4 10^{-6} cm/s	1.37 10^{-6} cm/s	18.9 10^{-6} cm/s
HLM Cl_{int} *in vitro*	<25 μL/min/mg	303 μL/min/mg	2433 μL/min/mg	ND
RLM Cl_{int} *in vitro*	<25 μL/min/mg	1672 μL/min/mg	11427 μL/min/mg	ND
logP	1 <logP< 3.5	3.2	4.5	3.1
Solubility (pH 7.4)	>50 μM	334 μM	18.4 μM	<5 μM
CYP51 IC_{50}	>10 μM	>10 μM	>10 μM	>10 μM

Figure 1. Chemical structures, biological data, and early ADME profiling of initial cyanopyridine hit compounds. Regions selected for SAR exploration, core: orange, linker: blue, RHS: magenta.

World Health Organization's (WHO) Special Programme for Research and Training in Tropical Diseases (TDR).[10] The main goal of this program was to contribute to reduce the translational and innovation gaps in disease endemic countries. The collaboration between the laboratory of Luiz Carlos Dias and TDR was first established in 2008. Later, Dias also joined forces with the Drugs for Neglected Diseases initiative (DNDi), a not-for-profit research and development global organization, to establish the LOLA consortium.[11] Coincidentally, DNDi also had a cyanopyridine series (hit PCBRO01-2472, Figure 1) derived from the HTS campaign performed by the Broad Institute using the NIH library (>300,000 compounds) against intracellular *T. cruzi* parasites.[12] While the optimization of all these series was done under the LOLA consortium, only the optimization of TDR30139 (**1**) will be shown here.

RESULTS AND DISCUSSION

After resynthesis of the initial hit TDR30139 (**1**), potency against intracellular *T. cruzi* amastigotes was reconfirmed (EC_{50} 1 μM), with good selectivity over MRC-5 cells (Table 1). In terms of chemical tractability, the synthesis of cyanopyridine derivatives is straightforward and economically feasible.[13−15] Considering this, a systematic structure−activity relationship (SAR) exploration was conducted to improve *in vitro* potency and selectivity and balance these with other *in vitro* ADME and physicochemical properties. To build this SAR, modifications were done in three main parts of the cyanopyridine series: the cyanopyridine core, linker, and right-hand side (RHS) substituents (Figure 1). Ultimately, 40 compounds, including the original hit, were designed, synthesized, and successfully tested using a structured screening cascade and relevant progression criteria.[16] Compounds were also screened against the other kinetoplastid parasites *Trypanosoma brucei*, *T.b. rhodesiense*, and *Leishmania infantum* (Table S1, Supporting Information).

The general strategy for synthesizing 3-cyanopyridines was to react thiopyridones and pyridones (**Ia−g**) with a variety of electrophiles (**II**) to afford the desired 2-thio-3-cyanopyridines **1−21**, **26−31** and 2-oxo-3-cyanopiridines **23** and **24**, respectively (Scheme 1). Phenol derivative **13** was obtained by hydrolysis of **12** using *p*-toluene sulfonic acid, while the 3-phenylamino analogue **22** was obtained by reduction of the corresponding 3-phenyl nitro precursor. Alkylation of **I-a** with 2-bromo-1-(3-methoxyphenyl)ethan-1-one followed by oxidation with *m*-chloroperoxybenzoic acid (mCPBA) led to sulfoxide **25**. Michael-like addition of the dimethylated thiopyridone (**I-a**) with enones (**III**) led to linker homologues **32** and **33**.

To further study linker modifications, a different strategy was followed for the synthesis of the 2-aza analogue **35**. Compound **34** was obtained through an aromatic nucleophilic substitution reaction on bromide **I-h** with 2-hydroxy-2-(4-fluorophenyl)ethylamine, followed by oxidation of the intermediate alcohol (**34**) to the ketone **35** (Scheme 2A). Replacement of the carbonyl group by a free amine (**37**) was achieved by nucleophilic addition of the bromoalkylazide to intermediate **I-a**, followed by reduction of the azide **36** (Scheme 2B). Compounds **38** and **39**, both bearing an amide group at position 3, were synthesized by condensing acetylacetone with 3-amino-3-thioxopropanamide, followed by alkylation of the resulting intermediate **I-i** with the respective chloroalkyl ketones (Scheme 2C). Compound **42**, bearing a tetrazole at position 3, was obtained through a [2 + 3] cycloaddition of the cyano intermediate **40** with sodium azide, followed by tetrazole alkylation and oxidation of the intermediate alcohol (**41**) to the corresponding ketone **42** (Scheme 2E). Finally, *S*-alkylation of pyrimidinethione **I−j** furnished an analogue lacking the cyano function at position 3 (**43**, Scheme 2E)

Initially, we focused our modifications on the RHS (Table 1). We found that replacing the 2-thiophene, present in **1**, with a phenyl (**2**) and the 3-regioisomer (**3**) did not impact hugely on potency. Alkylated phenyl substituents (**4**, **5**) were well tolerated, providing a potency boost at the expense of increasing lipophilicity (EC_{50} 0.08 and 0.29 μM, respectively).

https://doi.org/10.1021/acsomega.4c01919
ACS Omega 2024, 9, 22360−22370

Table 1. Exploration of Right-Hand-Side SAR

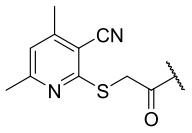

Compound	R	*T. cruzi* EC_{50} (μM)[a]	MRC-5 CC_{50} (μM)[b]	SI[c]	clogP[d]
1		1.00	> 32.0	> 28	3.16
2		0.74	> 64.0	> 102	3.48
3		1.06	> 64.0	> 53	3.16
4		0.08	> 64.0	> 966	3.89
5	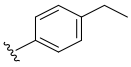	0.29	> 64.0	> 141	4.22
6	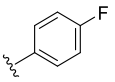	0.63	> 64.0	> 102	3.64
7	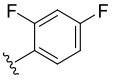	0.56	36.2	65	3.69
8	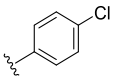	0.33	> 64.0	> 227	4.04
9	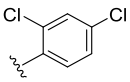	0.14	> 64.0	> 524	4.55
10	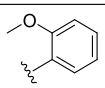	3.64	> 61.3	> 23	3.43
11	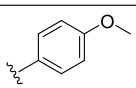	1.56	24.0	19	3.42
12	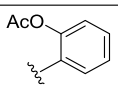	1.50	12.4	9	3.34
13	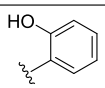	3.10	> 64.0	> 30	3.61
14		2.08	7.20	3	2.39
15	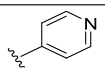	> 64.0	> 56.3	–	2.39
16	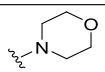	48.9	29.5	0.7	1.14
17	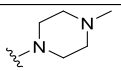	> 64.0	> 64.0	–	1.18
22	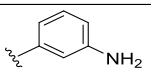	6.89	> 64.0	> 9	2.92

[a]EC_{50} values against *T. cruzi* represent the mean of two individual experiments. EC_{50} of benznidazole (positive control) was 3.1 μM. [b]CC_{50} values represent the mean of two individual experiments. [c]Selectivity index (SI) = CC_{50} MRC-5/EC_{50} *T. cruzi*. [d]*c* log *P* values were calculated by StarDrop V7.5.0.38968 (www.optibrium.com).

https://doi.org/10.1021/acsomega.4c01919
ACS Omega 2024, 9, 22360−22370

Scheme 1. Synthesis of Cyanopyridine Derivatives 1−33[a]

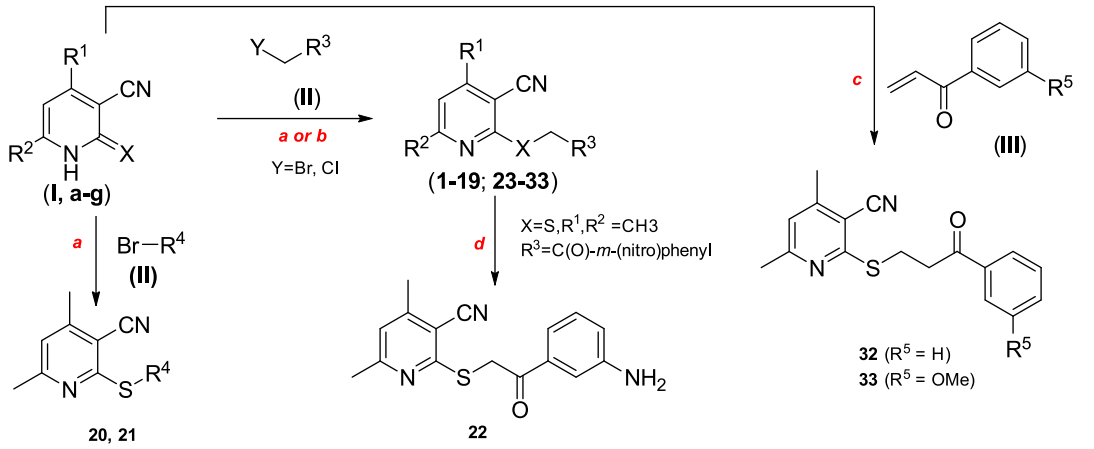

X=S; R^1,R^2 =CH_3

1 R^3=C(O)-2-thiophenyl
2 R^3=C(O)-phenyl
3 R^3=C(O)-3-thiophenyl
4 R^3=C(O)-*o*-(methyl)phenyl
5 R^3=C(O)-*p*-(ethyl)phenyl
6 R^3=C(O)-*p*-(fluor)phenyl
7 R^3=C(O)-2,4-di-fluorphenyl
8 R^3=C(O)-*p*-(chloro)phenyl
9 R^3=C(O)-2,4-di-chlorophenyl
10 R^3=C(O)-*o*-(methoxy)phenyl
11 R^3=C(O)-*p*-(methoxy)phenyl
12 R^3=C(O)-*o*-(O-acetyl)phenyl
13 R^3=C(O)-*o*-(hydroxy)phenyl
14 R^3=C(O)-2-pyridyl
15 R^3=C(O)-4-pyridyl
16 R^3=C(O)N(CH_2CH_2)$_2$O
17 R^3=C(O)N(CH_2CH_2)$_2$NCH_3
18 R^3=phenyl
19 R^3=C(O)NHphenyl
20 R^4=CH(CH_3)-C(O)-phenyl
21 R^4=chroman-4-one

X=O; R^1,R^2 =CH_3

23 R^3=C(O)-phenyl
24 R^3=C(O)-*m*-(methoxy)phenyl

25 X=S(O); R^1, R^2=CH_3; R^3=C(O)-*m*-(methoxy)phenyl
26 X=S; R^1,R^2 =H; R^3=C(O)-*p*-(fluor)phenyl
27 X=S; R^1=methoxy; R^2=H; R^3=C(O)-phenyl
28 X=S; R^1=CH_3; R^2= methoxy; R^3=C(O)-phenyl
29 X=S; R^1=$NHCH_3$; R^2=H; R^3=C(O)-phenyl
30 X=S; R^1=CF_3; R^2= CH_3; R^3=C(O)-phenyl
31 X=S; R^1=CF_3; R^2= OH; R^3=C(O)-*p*-(methoxy)phenyl

I-a: X=S; R^1, R^2= CH_3
I-b: X=O, R^1, R^2= CH_3
I-c: X=S, R^1, R^2= H
I-d: X=S, R^1=methoxy, R^2= H
I-e: X=S; R^1=$NHCH_3$; R^2=H
I-f: X=S; R^1=CF_3; R^2= CH_3
I-g: X=S; R^1=CF_3; R^2= OH

[a]Reagents and conditions: (a) X = S, Et_3N, DCM, 0 °C, 2 h; (b) X = O, K_2CO_3, DCM, TBA-Br, H_2O, 45 °C, 20 min; (c) Et_3N, AcOH, THF, rt, 20 min; (d) Fe, AcOH, HCl, EtOH, reflux, 2 h; (e) p-TsOH, MeOH, rt, 2 h. For the synthesis of compounds **Ia**−**Ig**, see Supporting Information.

We also explored fluorinated derivatives since this moiety is well-known to successfully improve metabolic stability due to its electron-withdrawing property, reducing its propensity to oxidative metabolism.[17] The 4-fluorophenyl (**6**) and 2,4-difluorophenyl (**7**) analogues showed a slight increase in potency at the expense of adding 0.5 *c* log *P*, and the latter compound started to show some cytotoxicity toward MRC-5 cells (CC_{50} 36.2 μM). Other halogens were also explored, with 2- and 2,4-dichlorophenyl substituted derivatives (**8**, **9**) showing submicromolar anti-*T. cruzi* activity (EC_{50} 0.33 and 0.14 μM, respectively). Isosteric replacements for the phenyl ring using 2-pyridyl (**14**) did not affect the potency (EC_{50} 2.08 μM), but the 4-pyridyl (**15**) analogue was completely inactive.

Aiming to reduce lipophilicity, we investigated the effects of polar substituents at the RHS, such as methoxy (**10**, **11**) and amino groups (**22**).[18] However, none of the modifications showed any potency improvement compared to the initial hit **2** (EC_{50} 0.74 μM). Although acetoxy substituted **12** was moderately potent (EC_{50} 1.50 μM), it was discarded due to its inherent instability in biological media; in fact, its hydrolysis product, phenol **13**, was slightly less potent (EC_{50} 3.10 μM). A further modification in the RHS explored the replacement of aromatic rings for sp^3-saturated rings.[19] Both the morpholine (**16**) and *N*-methyl piperazine (**17**) derivatives were inactive. Additionally, **16** was slightly more cytotoxic (CC_{50} 29.5 μM) than initial hits (**1**, **2**). These results corroborate the previous aromatic SAR exploration, which suggested that only hydrophobic substituents are tolerated and polar substituents at the RHS lead to inactive compounds.

To analyze the importance of the linker region for anti-*T. cruzi* activity, analogues with modifications focusing on the carbonyl function, the methylene spacer, and the heteroatom were planned and synthesized (Table 2). Molecular simplification showed that the carbonyl group is key for activity since its removal abolished activity (**18**, EC_{50} 36.8 μM). Additionally, replacing the carbonyl group with polar functionalities, as in compounds **19**, **34**, and **37**, reduced lipophilicity (*c* log *P* 1.95−2.9) but compromised trypanocidal activity.

https://doi.org/10.1021/acsomega.4c01919
ACS Omega 2024, 9, 22360−22370

Scheme 2. Synthesis of Cyanopyridine Derivatives 34−43[a]

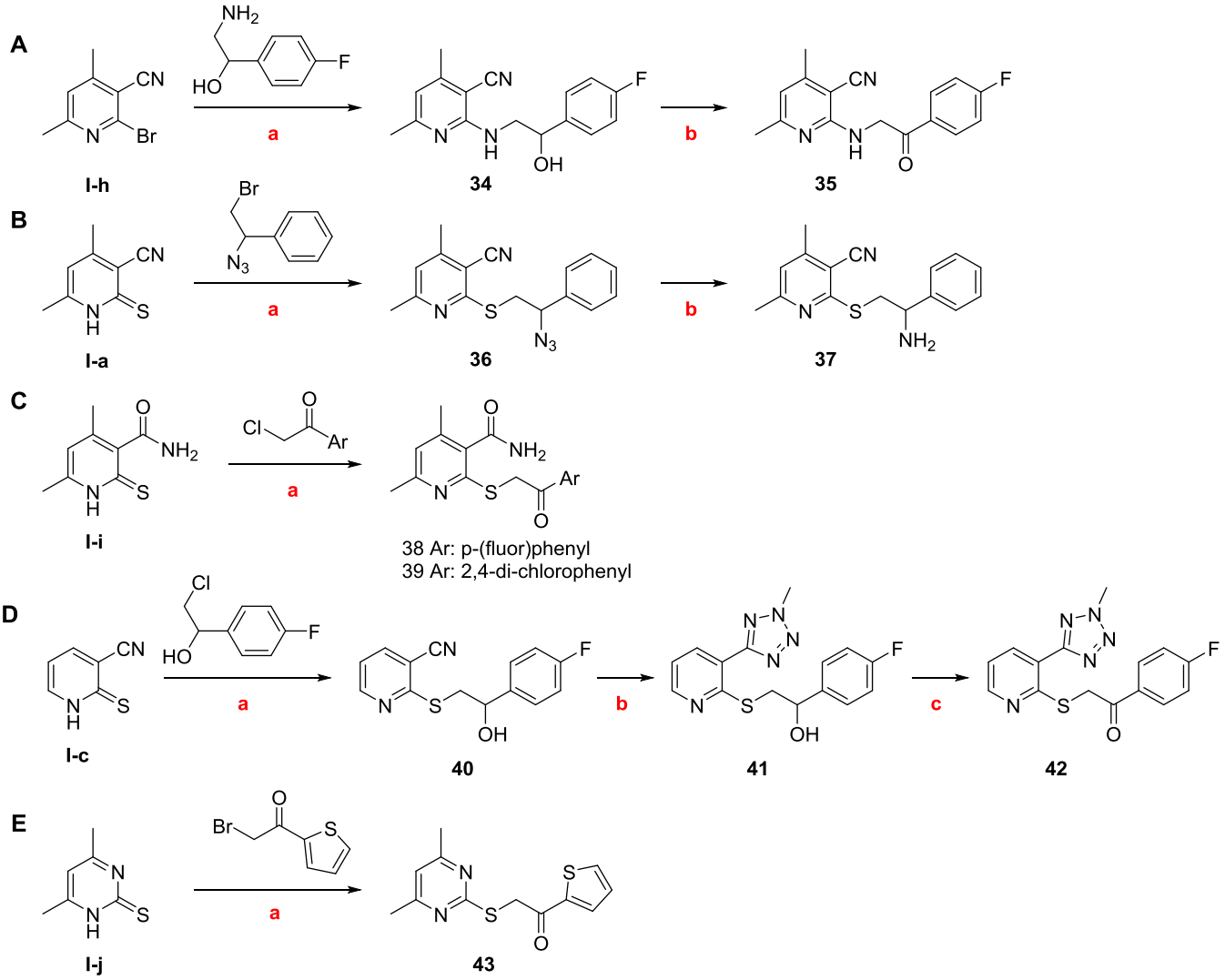

[a]Reagents and conditions: (A): (a) DIPEA, EtOH, reflux, 48 h; (b) PCC, DCM, rt, 5 h; (B): (a) THF, pyridine, KOH, 40 °C, 20 h; (b) PtO_2, $H_{2(g)}$, $NaHCO_3$, MeOH, THF, rt, 7 h; (C): (a) Et_3N, MeOH, rt, 2 h; (D) (a) DBU, THF, reflux, overnight; (b) NaN_3, TEA·HCl, toluene, reflux, 8 h; then $(CH_3O)_2SO_2$, K_2CO_3, acetone, rt, 2 h; (c) PCC, DCM, rt, 5 h. (E): (a) Et_3N, EtOH, 0 °C, 2 h. For the synthesis of compounds **I−h** to **I−j**, see Supporting Information.

Branching the linker with a methyl group (**20**) or homologation with methylene in the spacer (**32**, **33**) reduced potency, but a conformationally restricted analogue (**21**) was tolerated, but increased toxicity toward host cells (CC_{50} 12.7 μM) was observed. Sulfur was found to be essential for bioactivity since its replacement with classical and nonclassical isosteres oxygen (**23**, **24**) or nitrogen (**35**) (EC_{50} 20.7, 21.9, and >64.0 μM respectively) resulted in a significant potency drop. Oxidation to sulfoxide (**25**) preserved the activity but induced toxicity (EC_{50} 1.17, CC_{50} 18.9 μM). These results showed that only minor modifications are acceptable in this region without affecting the potency and toxicity profile.

After establishing the SAR around the linker and RHS regions, we explored modifications to the core (Table 3). Methyl groups at 4 and 6 positions were shown to be important for trypanocidal activity since the demethylated analogue **26** (EC_{50} 5.51 μM) was less potent compared with its corresponding match pair **6** (EC_{50} 0.63 μM). Incorporation of electron-donating groups into the 2 and 4-positions in the cyanopyridine core, such as methoxy (**27**, **28**) or methylamine (**29**) groups, was also tolerated (EC_{50} 5.39, 5.05, and 1.91 μM respectively); the methylamine was more potent and selective toward human cells compared to the methoxy derivatives (CC_{50} 52.9, 24.9, and >64 μM, respectively). Since the methyl groups provide benzylic positions, which are prone to oxidative metabolism, we sought to replace one of them with a trifluoro methyl group (**30**); this was detrimental to potency (EC_{50} 7.83 μM). Additionally, the concomitant introduction of the trifluoro methyl group and the pyridone function in compound **31** had an even more deleterious effect on potency (EC_{50} 15.4 μM).

We also synthesized carboxamides **38** and **39**, which have an alternative site for polar interactions at position 3. Both protic analogues showed reduced activity when compared to the original cyano compounds (EC_{50} 18.3 and 12.0 μM, respectively). Similarly, we replaced the original nitrile at position 3 with a methylated tetrazole group (**42**), which was completely devoid of antiparasitic activity. Abstracting the

https://doi.org/10.1021/acsomega.4c01919
ACS Omega 2024, 9, 22360−22370

Table 2. Exploration of the Linker SAR

Compound	Linker	RHS	*T. cruzi* EC_{50}[a]	MRC-5 CC_{50}[b]	SI[c]	clogP[d]
18	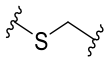		36.9	> 64.0	> 3	3.79
19	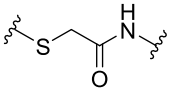		> 64.0	> 64.0	–	2.90
20	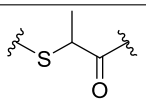		32.9	> 64.0	> 2	3.90
21	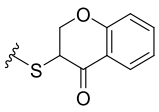		4.80	12.7	5	3.18
23	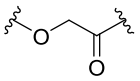		20.7	30.8	3	2.80
24	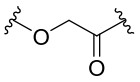	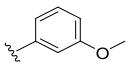	21.9	> 64.0	> 5	2.82
25	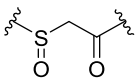	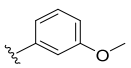	1.20	18.9	22	1.94
32	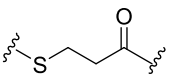		25.0	–	–	3.67
33	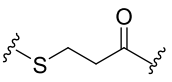	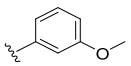	18.0	–	–	3.60
34	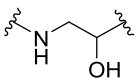	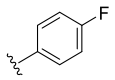	33.3	26.5	0.8	1.95
35	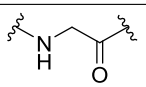	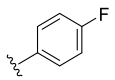	> 64.0	> 64.0	–	2.51
37	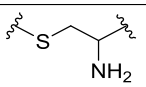		19.5	> 64.0	5	2.65

[a]EC_{50} values against *T. cruzi* represent the mean of two individual experiments. EC_{50} of benznidazole (positive control) was 3.1 μM. [b]CC_{50} values represent the mean of two individual experiments. [c]Selectivity index (SI) = CC_{50} MRC-5/EC_{50} *T. cruzi*. [d]*c* log *P* values were calculated by StarDrop V7.5.0.38968 (www.optibrium.com).

cyano group and replacing the pyridyl with a pyrimidine core (**43**) also resulted in inactivity. These results led us to conclude that only a few substituents and modifications on the core can be tolerated, with the cyano group and the sulfur atom being essential for activity. Furthermore, the addition of methyl groups provided a moderate increment in activity, most likely by increasing the lipophilicity of the molecules.

After analyzing potency and cytotoxicity, we selected 13 representative compounds for *in vitro* ADME profiling (Table 4). Most of the compounds had good passive permeability values; however, both human and mouse liver microsomal clearance (HLM/MLM) data showed that all compounds are metabolically unstable and contrary to the initial data, and they also have poor solubility. All compounds bearing aromatic substituents at the RHS suffered from extensive metabolism compared to the sp^3-ring morpholinyl (**16**) (HLM 32, MLM 73.9 μL/min/mg). This data is consistent with *in silico* calculations using the StarDrop P450 module, which pointed out possible soft spots, mainly on the core benzylic positions, sulfur linker, and aromatic RHS, as shown in Figure S1 (Supporting Information). This lower metabolic stability would almost certainly limit their oral exposure in animal models, so at this point, it was decided not to pursue *in vivo* studies, *i.e.*, pharmacokinetic, exploratory toxicology, or an efficacy model.

In summary, we found that aromatic substituents in the RHS are preferred while insertion of saturated heterocycles leads to inactive compounds. When exploring the linker, a better potency profile was observed when sulfur was present rather than oxygen or nitrogen, whereas no potency improvement was observed branching the linker or homologating. Additionally, the carbonyl group in the linker was essential for activity since its replacement or removal significantly reduced the potency. Furthermore, exploration of the core showed that the

https://doi.org/10.1021/acsomega.4c01919
ACS Omega 2024, 9, 22360−22370

Table 3. Exploration of the Core Scaffold SAR

Compound	Structure	*T. cruzi* EC_{50}[a]	MRC-5 CC_{50}[b]	SI[c]	clogP[d]
26	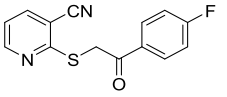	5.51	> 52.9	> 13	2.80
27	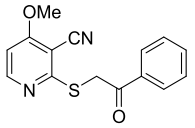	5.39	24.9	7	2.58
28	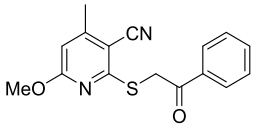	5.05	2.5	0.6	3.01
29	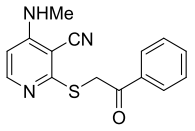	1.91	> 64.0	> 37	2.11
30	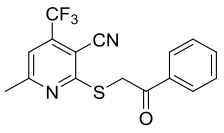	7.83	> 64.0	> 8	4.28
31	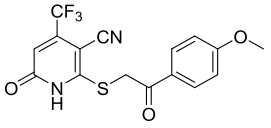	15.4	56.8	1	2.96
38	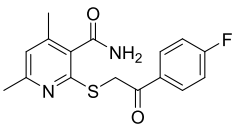	12.0	> 64.0	> 6	2.62
39	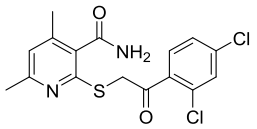	18.3	> 64.0	> 3	3.55
42	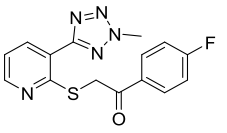	>64.0	> 64.0	–	2.26
43	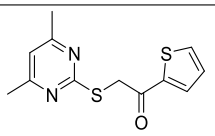	> 64.0	> 64.0	–	3.50

[a]EC_{50} values against *T. cruzi* represent the mean of two individual experiments. EC_{50} of benznidazole (positive control) was 3.1 μM. [b]CC_{50} values represent the mean of two individual experiments. [c]Selectivity index (SI) = CC_{50} MRC-5/EC_{50} *T. cruzi*. [d]*c* log *P* values were calculated by StarDrop V7.5.0.38968 (www.optibrium.com).

cyanopyridine substituent was essential for antiparasitic activity, and its replacement by a carboxamide or tetrazole did not improve potency, neither did replacement of the 3-cyanopyridine by a pyrimidine. Different substitution patterns on the pyridine were tolerated, but none of them had better potency than the initial hits. A comprehensive representation of the SAR is illustrated in Figure 2.

To help understand the SAR, we built a qualitative structure−activity relationship model using the Activity Atlas module available in Forge V10.6.0 (details in Supporting Information).[20] The regions explored are illustrated with negative and positive electrostatic fields, hydrophobicity, and shape (Figure 3A,B). Moving to active molecules, the proposed model highlights the regions, which were considered critical for potency (Figure 3C), in consonance with our previous SAR analysis. The key negative electrostatics took place in the nitrile of the core and the carbonyl group in the linker. Favorable hydrophobicity appeared at sulfur in the linker. In the RHS part, the model suggested that positive electrostatics and hydrophobicity were essential for activity and

https://doi.org/10.1021/acsomega.4c01919
ACS Omega 2024, 9, 22360−22370

Table 4. ADME Properties of Representative 3-Cyanopyridines Synthesized

Compound	Structure	HLM[a]	MLM[b]	PAMPA[c]	Solubility (μM)
1	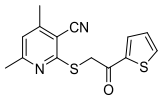	758	3480	25.4	< 5
2	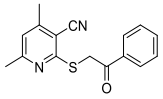	735	1560	20.4	< 5
3	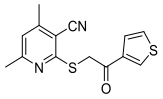	541	1320	23.3	< 5
5	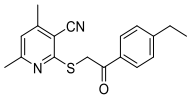	1070	8860	1.0	< 5
6	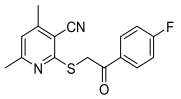	479	ND[d]	8.0	< 5
7	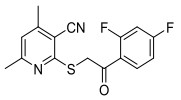	690	4040	7.5	< 5
8	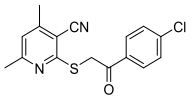	620	8880	4.3	< 5
9	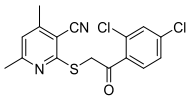	802	35300	1.7	< 5
10	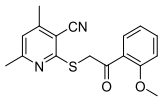	2030	9670	9.3	< 5
11	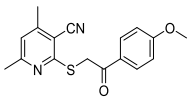	438	4300	24.6	< 5
16	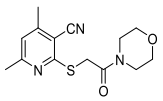	32	73.9	11.7	113
23	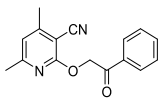	342	3240	31.1	34
38	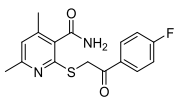	< 23.1	892	17.5	286

[a]HLM: Human liver microsome intrinsic clearance (μL/min/mg). [b]MLM: Mouse liver microsome intrinsic clearance (μL/min/mg). [c]Parallel artificial membrane permeability assay (PAMPA) effective permeability: 10^{-6} cm/s. [d]ND = not determined.

https://doi.org/10.1021/acsomega.4c01919
ACS Omega 2024, 9, 22360−22370

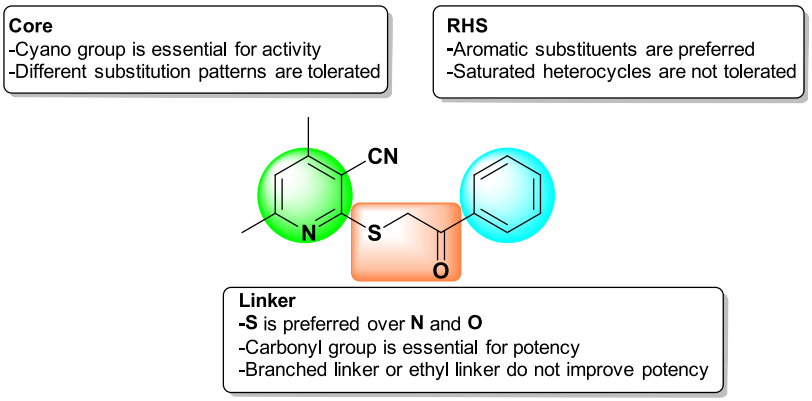

Figure 2. Structure−activity relationship of 3-cyanopyridine derivatives.

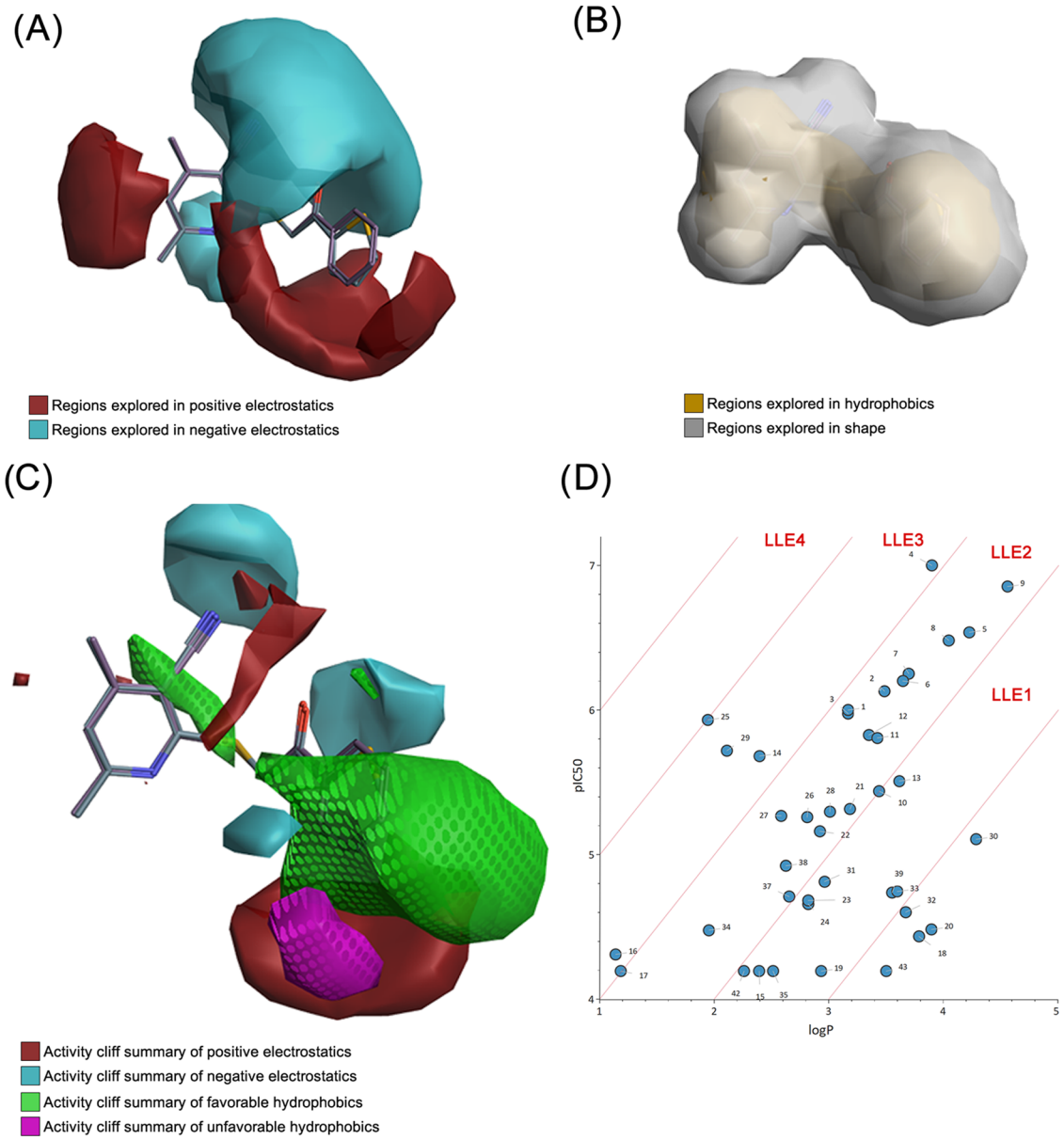

Figure 3. 3D-qualitative structure−activity relationship model using Activity Atlas in Forge 10.6.0. (A) Field regions explored in the data set. (B) Hydrophobicity and shape explored regions. (C) Summary of field regions of active compounds. (D) LLE plot of 3-cyanopyrdine derivatives.

https://doi.org/10.1021/acsomega.4c01919
ACS Omega 2024, 9, 22360−22370

led to initial predictions about correlations between potency and lipophilicity. To further understand this correlation, we analyzed the ligand lipophilicity efficiency (LLE, pEC_{50}-*c* log *P*), which is represented by the parallel lines in Figure 3D. This parameter correlates the potency to the lipophilicity of a compound. High-quality compounds, *i.e.*, those with a potency not driven mainly by nonspecific hydrophobic interactions, should be in the upper left of the graphic.[21] The set of compounds synthesized for the cyanopyridine series showed LLE values that could not be improved above 4 during the optimization process: it was not possible to improve the potency and, at the same time, lower the lipophilicity. This outcome corroborated the initial prediction that potency is mainly driven by lipophilicity within this set of compounds. Additionally, lipophilicity negatively impacts metabolic stability and solubility, which made further optimization of the series more difficult.

CONCLUSIONS

In conclusion, a series of cyanopyridine derivatives was synthesized and its anti-*T. cruzi* activity was established. For selected compounds, additional physicochemical and ADME properties were experimentally determined. A detailed SAR analysis revealed that the nitrile group in the core scaffold is crucial for potency, and variation in the thioether linker is not tolerated. Additionally, the presence of an acetophenone-like carbonyl group in the RHS is mandatory for potency. This series showed good potency and selectivity against *T. cruzi* and may represent a new class of compounds useful in the search for a new antiparasitic drug candidate. Unfortunately, we could not achieve balanced potency and physicochemical properties. Despite our efforts to optimize hit compounds, it proved difficult to make compounds with LLE above 4, since, within this series, potency is driven mainly by lipophilicity and higher log *P* values are usually associated with poor metabolic stability and solubility. Thus, it was decided to stop further work on this series. This study could provide new insights about high-quality hit compounds for Chagas disease that could be used as probes to identify new drug targets in *T. cruzi*.

ASSOCIATED CONTENT

Supporting Information

The Supporting Information is available free of charge at https://pubs.acs.org/doi/10.1021/acsomega.4c01919.

NMR (^{1}H and ^{13}C) characterization; high-resolution mass spectra; and experimental details regarding organic synthesis; kinetic solubility; PAMPA; microsomal stability; biology procedures; additional parasite screening; and molecular modeling (PDF)

Molecular formula strings (XLSX)

AUTHOR INFORMATION

Corresponding Author

Luiz C. Dias − *Institute of Chemistry, State University of Campinas, Campinas 13083-970 São Paulo, Brazil;* orcid.org/0000-0003-0628-9928; Email: ldias@unicamp.br

Authors

Brian W. Slafer − *Institute of Chemistry, State University of Campinas, Campinas 13083-970 São Paulo, Brazil;* orcid.org/0009-0003-5655-1848

Marco A. Dessoy − *Institute of Chemistry, State University of Campinas, Campinas 13083-970 São Paulo, Brazil;* orcid.org/0009-0005-5731-761X

Ramon G. de Oliveira − *Institute of Chemistry, State University of Campinas, Campinas 13083-970 São Paulo, Brazil;* orcid.org/0000-0002-2407-5766

Maria C. Mollo − *Institute of Chemistry, State University of Campinas, Campinas 13083-970 São Paulo, Brazil;* orcid.org/0000-0001-8040-2533

Eun Lee − *Institute of Chemistry, State University of Campinas, Campinas 13083-970 São Paulo, Brazil;* orcid.org/0000-0001-6893-4799

An Matheeussen − *Laboratory of Microbiology, Parasitology and Hygiene, University of Antwerp, Antwerp 2000, Belgium*

Louis Maes − *Laboratory of Microbiology, Parasitology and Hygiene, University of Antwerp, Antwerp 2000, Belgium*

Guy Caljon − *Laboratory of Microbiology, Parasitology and Hygiene, University of Antwerp, Antwerp 2000, Belgium;* orcid.org/0000-0002-4870-3202

Leonardo L. G. Ferreira − *Laboratory of Medicinal and Computational Chemistry, Physics Institute of Sao Carlos, University of Sao Paulo, Sao Carlos 13566-590 São Paulo, Brazil;* orcid.org/0000-0002-6947-0639

Renata Krogh − *Laboratory of Medicinal and Computational Chemistry, Physics Institute of Sao Carlos, University of Sao Paulo, Sao Carlos 13566-590 São Paulo, Brazil;* orcid.org/0000-0002-6545-608X

Adriano D. Andricopulo − *Laboratory of Medicinal and Computational Chemistry, Physics Institute of Sao Carlos, University of Sao Paulo, Sao Carlos 13566-590 São Paulo, Brazil;* orcid.org/0000-0002-0457-818X

Luiza R. Cruz − *Drugs for Neglected Diseases initiative, Geneva 1202, Switzerland;* orcid.org/0000-0001-6103-9345

Charles E. Mowbray − *Drugs for Neglected Diseases initiative, Geneva 1202, Switzerland;* orcid.org/0000-0003-3538-8116

Jadel M. Kratz − *Drugs for Neglected Diseases initiative, Geneva 1202, Switzerland;* orcid.org/0000-0002-7681-8234

Complete contact information is available at: https://pubs.acs.org/10.1021/acsomega.4c01919

Author Contributions

[⊥]M.A.D. and B.W.S. authors contributed equally. M.A.D. and B.W.S. carried out design and synthetic chemistry efforts; R.G.O., E.L., and M.C.M. carried out analytic and computational chemistry efforts; A.M., L.M., G.C., L.L.G.F., and R.K. carried out biological experiments; A.D.A., L.R.C., C.E.M., J.M.K., and L.C.D. conceived experiments, provided guidance about data interpretation and design of compounds; J.M.K., A.D.A., and L.C.D. conceived and planned the project. All authors contributed to the manuscript writing. The manuscript was written through the contributions of all authors. All authors approved the final version of the manuscript.

Funding

R.G.O., E.L., and M.C.M. are supported by FAPESP (grants no. 2018/24344-4, 2021/02761-5, 2020/10493-8). L.C.D., A.D.A., and L.L.G.F receive support from FAPESP grant no. 2013/07600-3 (CIBFar-CEPID-FAPESP) and FAPESP-PITE grant no. 2015/50655-9. For this work, DNDi received financial support from the Ministry of Health of Brazil, the

Swiss Agency for Development and Cooperation (SDC), Switzerland; Dutch Ministry of Foreign Affairs (DGIS), The Netherlands; UK International Development, UK, and other private foundations and individuals.

Notes

The authors declare no competing financial interest.

■ ACKNOWLEDGMENTS

The authors further thank UNICAMP NMR and technical staff for assistance; the teams at the Swiss Tropical and Public Health Institute (Dr. Marcel Kaiser) and AbbVie for in-kind secondary profiling of compounds, and Dr. Dale Kempf (AbbVie) and Dr. Michael Schrimpf (AbbVie) for helpful discussions. The authors are also grateful to Cresset for providing the academic license for Flare and Forge. DNDi is grateful to its donors, public and private, who have provided funding for all DNDi activities since its inception in 2003. A full list of DNDi's donors can be found at http://www.dndi.org/donors/donors/.

■ ABBREVIATIONS

PAMPA, parallel artificial membrane permeability assay; CD, Chagas disease; NCE, new chemical entity; DNDi, Drugs for Neglected diseases initiative; LOLA, Lead Optimization Latin America; ADME, absorption, distribution, metabolism, excretion; SAR, structure−activity relationships

■ REFERENCES

(1) WHO. Chagas disease - World Health Organization. https://www.who.int/health-topics/chagas-disease. (accessed June 13, 2023).
(2) PAHO. Chagas disease - Pan American Health Organization. https://www.paho.org/en/topics/chagas-disease. (accessed June 13, 2023).
(3) Junior, P. A.; Molina, I.; Murta, S. M.; Sánchez-Montalvá, A.; Salvador, F.; Corrêa-Oliveira, R.; Carneiro, C. M. Experimental and Clinical Treatment of Chagas Disease: A Review. *Am. J. Trop. Med. Hyg.* **2017**, *97* (5), 1289−1303.
(4) Müller Kratz, J.; Garcia Bournissen, F.; Forsyth, C. J.; Sosa-Estani, S. Clinical and Pharmacological Profile of Benznidazole for Treatment of Chagas Disease. *Expert Rev. Clin. Pharmacol.* **2018**, *11* (10), 943−957.
(5) Torrico, F.; Gascón, J.; Barreira, F.; Blum, B.; Almeida, I. C.; Alonso-Vega, C.; Barboza, T.; Bilbe, G.; Correia, E.; Garcia, W.; Ortiz, L.; Parrado, R.; Ramirez, J. C.; Ribeiro, I.; Strub-Wourgaft, N.; Vaillant, M.; Sosa-Estani, S.; Arteaga, R.; de la Barra, A.; Camacho Borja, J.; Martinez, I.; Fernandes, J.; Garcia, L.; Lozano, D.; Palacios, A.; Schijman, A.; Pinazo, M. J.; Pinto, J.; Rojas, G.; Estevao, I.; Ortega-Rodriguez, U.; Mendes, M. T.; Schuck, E.; Hata, K.; Maki, N.; Asada, M. New Regimens of Benznidazole Monotherapy and in Combination with Fosravuconazole for Treatment of Chagas Disease (BENDITA): A Phase 2, Double-Blind, Randomised Trial. *Lancet Infect. Dis.* **2021**, *21* (8), 1129−1140.
(6) Morillo, C. A.; Marin-Neto, J. A.; Avezum, A.; Sosa-Estani, S.; Rassi, A.; Rosas, F.; Villena, E.; Quiroz, R.; Bonilla, R.; Britto, C.; Guhl, F.; Velazquez, E.; Bonilla, L.; Meeks, B.; Rao-Melacini, P.; Pogue, J.; Mattos, A.; Lazdins, J.; Rassi, A.; Connolly, S. J.; Yusuf, S. Randomized Trial of Benznidazole for Chronic Chagas' Cardiomyopathy. *N. Engl. J. Med.* **2015**, *373* (14), 1295−1306.
(7) Torrico, F.; Gascon, J.; Ortiz, L.; Alonso-Vega, C.; Pinazo, M.-J.; Schijman, A.; Almeida, I. C.; Alves, F.; Strub-Wourgaft, N.; Ribeiro, I.; Santina, G.; Blum, B.; Correia, E.; Garcia-Bournisen, F.; Vaillant, M.; Morales, J. R.; Pinto Rocha, J. J.; Rojas Delgadillo, G.; Magne Anzoleaga, H. R.; Mendoza, N.; Quechover, R. C.; Caballero, M. Y. E.; Lozano Beltran, D. F.; Zalabar, A. M.; Rojas Panozo, L.; Palacios Lopez, A.; Torrico Terceros, D.; Fernandez Galvez, V. A.; Cardozo, L.; Cuellar, G.; Vasco Arenas, R. N.; Gonzales, I.; Hoyos Delfin, C. F.; Garcia, L.; Parrado, R.; de la Barra, A.; Montano, N.; Villarroel, S.; Duffy, T.; Bisio, M.; Ramirez, J. C.; Duncanson, F.; Everson, M.; Daniels, A.; Asada, M.; Cox, E.; Wesche, D.; Diderichsen, P. M.; Marques, A. F.; Izquierdo, L.; Sender, S. S.; Reverter, J. C.; Morales, M.; Jimenez, W. Treatment of Adult Chronic Indeterminate Chagas Disease with Benznidazole and Three E1224 Dosing Regimens: A Proof-of-Concept, Randomised, Placebo-Controlled Trial. *Lancet Infect. Dis.* **2018**, *18* (4), 419−430.
(8) Molina, I.; Gómez i Prat, J.; Salvador, F.; Treviño, B.; Sulleiro, E.; Serre, N.; Pou, D.; Roure, S.; Cabezos, J.; Valerio, L.; Blanco-Grau, A.; Sánchez-Montalvá, A.; Vidal, X.; Pahissa, A. Randomized Trial of Posaconazole and Benznidazole for Chronic Chagas' Disease. *N. Engl. J. Med.* **2014**, *370* (20), 1899−1908.
(9) Beltran-Hortelano, I.; Alcolea, V.; Font, M.; Pérez-Silanes, S. Examination of Multiple Trypanosoma Cruzi Targets in a New Drug Discovery Approach for Chagas Disease. *Bioorg. Med. Chem.* **2022**, *58*, No. 116577.
(10) Lead Discovery for Infectious Tropical Diseases - Annual Report 2009. World Health Organization and TDR for Research on Diseases of Poverty. https://tdr.who.int/docs/librariesprovider10/meeting-reports/tdr-bl3-10-eng-pdf.pdf. (accessed Nov 24, 2023).
(11) LOLA: DNDi's First Innovative Neglected Disease Early-Stage Research Programme Launches in Latin America. https://dndi.org/news/2013/first-early-stage-research-latin-america/. (accessed Nov 24, 2023).
(12) Andriani, G.; Chessler, A.-D. C.; Courtemanche, G.; Burleigh, B. A.; Rodriguez, A. Activity In Vivo of Anti-Trypanosoma Cruzi Compounds Selected from a High Throughput Screening. *PLoS Neglected Trop. Dis.* **2011**, *5* (8), No. e1298.
(13) Wenlock, M. C.; Austin, R. P.; Barton, P.; Davis, A. M.; Leeson, P. D. A Comparison of Physiochemical Property Profiles of Development and Marketed Oral Drugs. *J. Med. Chem.* **2003**, *46* (7), 1250−1256.
(14) Keserü, G. M.; Makara, G. M. The Influence of Lead Discovery Strategies on the Properties of Drug Candidates. *Nat. Rev. Drug Discovery* **2009**, *8* (3), 203−212.
(15) Hopkins, A. L.; Keserü, G. M.; Leeson, P. D.; Rees, D. C.; Reynolds, C. H. The Role of Ligand Efficiency Metrics in Drug Discovery. *Nat. Rev. Drug Discovery* **2014**, *13* (2), 105−121.
(16) Kratz, J. M.; Gonçalves, K. R.; Romera, L. M.; Moraes, C. B.; Bittencourt-Cunha, P.; Schenkman, S.; Chatelain, E.; Sosa-Estani, S. The Translational Challenge in Chagas Disease Drug Development. *Mem. Inst. Oswaldo Cruz* **2022**, *117*, e200501.
(17) Stepan, A. F.; Mascitti, V.; Beaumont, K.; Kalgutkar, A. S. Metabolism-Guided Drug Design. *MedChemComm* **2013**, *4* (4), 631−652.
(18) Miller, R. R.; Madeira, M.; Wood, H. B.; Geissler, W. M.; Raab, C. E.; Martin, I. J. Integrating the Impact of Lipophilicity on Potency and Pharmacokinetic Parameters Enables the Use of Diverse Chemical Space during Small Molecule Drug Optimization. *J. Med. Chem.* **2020**, *63* (21), 12156−12170.
(19) Subbaiah, M. A. M.; Meanwell, N. A. Bioisosteres of the Phenyl Ring: Recent Strategic Applications in Lead Optimization and Drug Design. *J. Med. Chem.* **2021**, *64* (19), 14046−14128.
(20) Cheeseright, T.; Mackey, M.; Rose, S.; Vinter, A. Molecular Field Extrema as Descriptors of Biological Activity: Definition and Validation. *J. Chem. Inf. Model.* **2006**, *46* (2), 665−676.
(21) Young, R. J.; Leeson, P. D. Mapping the Efficiency and Physicochemical Trajectories of Successful Optimizations. *J. Med. Chem.* **2018**, *61* (15), 6421−6467.

https://doi.org/10.1021/acsomega.4c01919
ACS Omega 2024, 9, 22360−22370